Strong localization of electrons in quasi-one-dimensional conductors

Yu. B. Khavin and M. E. Gershenson
Department of Physics and Astronomy, Serin Physics Laboratories, Rutgers University, Piscataway, New Jersey 08854-8019

A. L. Bogdanov
Lund University, MAX-lab, National Laboratory, S-221 00 Lund, Sweden

(Received 7 May 1998)

We report on an experimental study of electron transport in submicrometer-wide ''wires'' fabricated from Si δ-doped GaAs. These quasi-one-dimensional (Q1D) conductors demonstrate the crossover from weak to strong localization with decreasing temperature. On the insulating side of the crossover, the resistance has been measured as a function of temperature, magnetic field, and applied voltage for different values of the electron concentration, which was varied by applying the gate voltage. The activation temperature dependence of the resistance has been observed with the activation energy close to the mean energy spacing of electron states within the localization domain. The study of nonlinearity of the current-voltage characteristics provides information on the distance between the critical hops that govern the resistance of Q1D conductors in the strong localization (SL) regime. We observe the exponentially strong negative magnetoresistance; this orbital magnetoresistance is due to the universal magnetic-field dependence of the localization length in Q1D conductors. The method of measuring the single-particle density of states (DOS) in the SL regime has been suggested. Our data indicate that there is a minimum of DOS at the Fermi level due to the long-range Coulomb interaction. [S0163-1829(98)03936-8]

I. INTRODUCTION

Recent progress in technology enables the realization of a wide variety of materials with one-dimensional (1D) structural and electronic properties: high-mobility heterojunction microstructures,[1] heavy-doped conjugated polymers,[2] carbon nanotubes,[3] or organic conductors,[4] to mention a few. Because of a very broad current usage of the term ''1D systems,'' the physical properties of these conductors are diverse. In the limit of one conducting channel (conductors with cross-sectional dimensions smaller than the Fermi wavelength of the conduction electrons), there is a strong unscreened interaction between electrons. The electron states are correlated along the channel, and the poorly defined single-electron excitations cannot be treated as Landau quasiparticles. The behavior of these so-called quantum ''wires'' is described by the Tomonaga-Luttinger model, and the ideas span from the Wigner crystal in the case of the long-range interactions to the charge-density waves for the short-range interactions (for recent reviews, see Refs. 4–7).

In this paper, we are concerned with another class of 1D conductors, usually referred to as quasi-one-dimensional (Q1D) conductors. In these disordered conductors, there are many channels with strong scattering between them, and the quasiparticle excitations are well described by the Fermi-liquid theory. The physics of these systems is essentially different from the physics of quantum wires. The electron mean free path l is much smaller than the length of these conductors, and the coherent scattering from many impurities gives rise to Anderson localization.[8] To be one dimensional with respect to the quantum interference effects, a conductor should have cross-sectional dimensions smaller than the length of localization of the electron wave function, ξ, and the phase-breaking length L_φ (for a review, see Ref. 9).

It is widely believed that all electron states in low-dimensional conductors are localized when both spin-orbit (SO) and electron-electron interactions are weak.[8,10] The localization length for a Q1D conductor with a large number of transverse channels N_{1D} and weak SO scattering can be expressed at $H=0$ as[11,12]

$$\xi = N_{1D} l = \frac{\pi\hbar}{e^2}\sigma_1, \tag{1}$$

where σ_1 is the conductance of a wire per unit length in the ''metallic'' regime. Despite of electron localization, this ''metallic'' conductance can be rather large at room temperature. This is due to strong inelastic scattering: the electron scatters to another state, localized around a different site, before it diffuses over the localization length [the weak localization (WL) regime]. However, with decreasing the temperature, a low-dimensional conductor should eventually become an insulator. Electron transport can proceed only by hopping in this strong localization (SL) regime.

Until recently, the temperature-driven crossover has been observed only in two-dimensional conductors.[13–16] In one-dimensional metal-oxide-semiconductor field-effect transistor (MOSFET) type structures, the transition to the insulating regime has been observed with decreasing the carrier concentration.[1] In this case, however, all electron parameters *and* disorder have been changed simultaneously with variation of the gate voltage, and the electron states were *quite different* in the ''metallic'' and insulating regimes.

The study of the crossover is more informative if the crossover is observed as a function of temperature: in this case the data obtained in the WL and SL regimes are perti-

TABLE I. Parameters of the samples.

	Sample No.					
	1	2	3	4	5	6
W (μm)	0.05	0.06	0.1	0.12	0.2	0.18
L (μm)	500	500	40	500	40	500
No. of parallel ''wires''	470[a]	470	5	470	5	470
$R_\square(T=20$ K), kΩ	1.6	1.7	3.5	1.6	4.2	1.7
ξ (μm)	0.40	0.46	0.37	1.0	0.61	1.4
Δ_ξ (K)	2.1	1.5	1.1	0.35	0.34	0.17
$T_0(H=0)$ (K)	2.6	1.87	1.47	0.42	0.39	0.2
$R_\xi(T=T_0)$ (kΩ)	20.4	21.3	28	23	24.4	24.3
H_ξ (kOe)	1.0	0.74	0.56	0.17	0.17	0.083
$H_\xi^{\rm expt}$ (kOe)	1.0	0.80	0.51	0.21	0.17	0.12
$H_\xi^{\rm expt}/T_0$ (kOe/K)	0.37	0.43	0.35	0.50	0.44	0.59

[a]Sample 1 has been scratched during the gate deposition, and after this it contained 360 wires.

nent to the *same* electron states. Though the theoretical prediction of this remarkable crossover in Q1D conductors was made by Thouless in 1977,[8] the experimental study of this fundamental problem was delayed for 20 years. The ''gap'' between the prediction and observation indicates that this is a very demanding experiment; in particular, the choice of adequate samples is crucial. Two objects that have been used extensively for the study of the WL regime, thin metal films and high-mobility heterostructures, do not suit well this purpose: the localization length in these conductors is too large, and, hence, the crossover temperature is too low for any conceivable cross section.[17,18]

Experiments[17,19,20] have demonstrated that the dominant decoherence mechanism in Q1D conductors at low temperatures is the quasielastic electron-electron scattering.[21] Analyzing these data, we came to a conclusion that the crossover temperature can be substantially increased by using low-mobility and heavily doped semiconductor structures. Recently we observed the *temperature-driven* crossover in submicrometer-wide ''wires'' fabricated from the Si δ-doped GaAs.[22–24] On the insulating side of the crossover, there remain unanswered questions that are crucial for understanding of the transport mechanisms in Q1D conductors. In this paper, we focus on the study of the conductivity of Q1D conductors in the strongly localized regime.

The paper is organized as follows. In Sec. II, we briefly describe the experimental technique and observation of the WL-SL crossover in our samples. The data obtained in the SL regime are discussed in Sec. III. Our experimental findings and conclusions are summarized in Sec. IV.

II. OBSERVATION OF THE WL-SL CROSSOVER

A. Samples

One can estimate the crossover temperature T_ξ using Thouless' idea that the localization length ξ and the phase-breaking length $L_\varphi(T_\xi)$ should be of the same order of magnitude at the crossover.[8] At low temperatures, the decoherence in Q1D conductors is due to the quasielastic electron-electron scattering (the so-called Nyquist decoherence mechanism).[21] The phase-breaking length in this case can be expressed as follows:[21]

$$L_\varphi=\left(\frac{\hbar^2 D\sigma_1}{\sqrt{2}e^2k_BT}\right)^{1/3}. \tag{2}$$

From comparison Eqs. (1) and (2), we obtain the following estimate;

$$T_\xi=\frac{e^2D}{\sqrt{2}\pi^2k_B\xi\sigma_1}\sim[DW^2(m^*)^2]^{-1}, \tag{3}$$

where D is the electron diffusion constant in the metallic regime, W is the width of a ''wire'' fabricated from two-dimensional electron gas, and m^* is the effective electron mass. Thus, one could expect larger T_ξ for *narrow disordered* conductors with a *small* effective mass of the current carriers.

We have used wires fabricated from δ-doped GaAs. The effective mass of electrons in these structures coincides with $m^*\simeq 0.067m_e$ in GaAs. A single δ-doped layer with concentration of Si donors $N_D=5\times10^{12}$ cm^{-2} is 0.1 μm beneath the surface of an undoped GaAs. Using the electron beam lithography and deep ion etching, we were able to prepare uniform conducting wires with the effective width W as small as 0.05 μm. Because of the side-wall depletion, the effective width is smaller than the ''geometrical'' one by 0.15–0.2 μm, depending on the carrier concentration. The values of W, obtained from the sample resistance, were in accord with the estimate of W from the analysis of the WL magnetoresistance. Parameters of the samples are listed in Table I.

For several samples, we repeated the whole set of measurements after deposition of a thin ($\sim$50 nm) silver film on top of the structure. This metal film was used as a gate electrode: by varying the gate voltage V_g, we could ''tune'' the carrier concentration and mobility, and, hence, the localization length. The metal film deposition also serves a different purpose: it modifies the Coulomb interaction at distances greater than the distance between the electron gas and the metal film $t=0.1$ μm, and allows one to test the effect of the electron-electron interactions on the conductivity in the SL regime.

The carrier concentration n in the wires could differ substantially from that in the 2D δ-doped layer because of the

side-wall depletion. The direct measurement of n (e.g., from the Shubnikov–de Haas oscillations) cannot be performed in these very disordered and narrow wires (see, e.g. Ref. 25). An indirect estimate of n can be done as follows. It is well established that the electron mobility μ in the δ-doped layers with $N_D=5\times10^{12}$ cm^{-2} is $\sim(1\pm0.2)\times10^3$ cm^2/V s.[26] Assuming that $\mu=10^3$ cm^2/V s in our samples, we obtain a reasonable estimate $n\approx3\times10^{12}$ cm^{-2} for $V_g=0$; this corresponds to $\sim$40% compensation of Si donors, which is typical for the δ-doped layers with $N_D=5\times10^{12}$ cm^{-2} (see, e.g., Ref. 27). For this carrier concentration, only the lowest 2D subband is occupied.[28] It is worth noting that the knowledge of the exact value of n *is not crucial* for most of the effects discussed below.

A relatively high concentration of carriers ensures that the number of transverse channels in our samples is large ($N_{1D}\approx7-30$). The localization length is always much greater than the mean free path l, and electron motion is *diffusive* within the localization domain. At high temperatures, these samples can be considered as a disordered two-dimensional metal with the Fermi energy ε_F of the order of $\sim10^3$ K, and the parameter k_Fl ranging from 6 to 40 (k_F is the Fermi wave number). In particular, the density of states for noninteracting electrons should be energy independent, as in two dimensions, because of the strong interchannel scattering ($\hbar/\tau\gg\varepsilon_F/N_{1D}$, where τ is the momentum relaxation time). However, at low temperatures the samples become *one dimensional* with respect to the quantum interference effects: $W<L_\varphi(T)\leqslant\xi$.

In these samples, the electrons are localized over a large area ξW, which is shared by several thousand of the other localized electrons. Though the electron states strongly overlap in space, they are separated by the mean energy spacing within the localization domain

$$\Delta_\xi(1\mathrm{D})=(\nu_{1D}\xi)^{-1}, \tag{4}$$

where ν_{1D} is the single-particle density of states (due to the strong interchannel scattering, $\nu_{1D}=W\nu_{2D}$). For the samples discussed in this paper, this energy spacing varies from 0.1 to 5 K depending on the wire width and the carrier concentration.

We studied the resistance of many wires connected in parallel. This has been done for two reasons. First, the parallel connection of wires enlarges the temperature interval where the sample resistance is within the range of our measuring equipment ($\leqslant1$ GΩ). Second, increasing the number of wires and their length reduces mesoscopic fluctuations by improving the ensemble averaging. Initially, we studied five 40 μm-long wires connected in parallel,[22] later the number of wires was increased up to 470, and the length L of each wire—up to 500 μm.[23,24] The distance between the wires is 1 μm in all the samples. The longer wires have an additional important advantage: the voltage interval that corresponds to the *linear* current-voltage (I-V) characteristics is narrow for our samples (see Sec. III), and the use of the longer wires facilitates measurements in the linear regime.

B. Measuring technique

For the measurements, we use a dilution refrigerator with a base temperature of 30 mK. All the wiring in the refrigerator is done by shielded twisted pairs of wires; the resistance between all the wires is much greater than 1 GΩ. An external noise pickup has been minimized by filtering of all the wires going into the cryostat.

We exploit two techniques for measuring the resistance. For $R\leqslant5$ MΩ, we have used a lock-in amplifier with an input resistance of 20 MΩ; a low measuring frequency ($f=0.5$ Hz) has been chosen because of large values of the sample resistance and capacitance of the filters. Due to a very high sensitivity of the lock-in technique, high-resolution resistance measurements can be done at low voltage levels ($V\sim10^{-6}$ V). This is an important advantage of the ac measurements, because the region of linearity of the I-V characteristics becomes narrower with increasing the localization length: e.g., for a sample with $\xi\sim1$ μm and $L=500$ μm the nonlinearity is observed at V as small as 10^{-4} V (see Sec. III). For the resistance measurements in the range 10 M$\Omega\leqslant R\leqslant1$ GΩ, we have used a dc current source and electrometer with the input resistance greater than 1×10^{14} Ω. The electrometer resolution, which was mostly limited by slow drifts, has been increased up to $\Delta V\sim1\times10^{-5}$ V by alternating of the measuring current direction.

C. Crossover from weak to strong localization

The resistance of all the samples increases with decreasing the temperature (Fig. 1). At high temperatures, a slow growth of R is consistent with the theory of quantum corrections to the resistance in the WL regime.[24] However, a dramatic change in the temperature dependence of the resistance has been observed for sufficiently narrow ($W<0.3$ μm) wires: it becomes activation-type at low temperatures.

We have shown that the Q1D conductors are driven into the insulating state by *both* single-particle localization and electron-electron interaction.[24] This evidence stems from the study of precursors of the crossover, namely, from the quantitative analysis of the temperature and magnetic field dependences of the resistance on the ''metallic'' side of the crossover. The contributions to the resistance due to localization and interaction effects are of the same order of magnitude at the crossover. The temperature dependence of the resistance is well described by the sum of the first-order quantum corrections down to $\sim3T_\xi$, where T_ξ is the crossover temperature; at lower temperatures, the higher-order corrections become important (see Sec. III A for our method of finding T_ξ).

Since our samples are driven into the insulating state by both localization and interaction effects, it is not obvious that the Thouless scenario, which has been suggested for a system of noninteracting electrons,[8] applies in this case. However, the experiment demonstrates that the features of the observed crossover are consistent with the Thouless predictions.

First, the resistance R_ξ, calculated for a wire segment of a length of ξ, is 24 ± 4 kΩ at the crossover temperature (see Table I and Fig. 1), which is close to the quantum resistance h/e^2 expected for such a wire in the vicinity of the Thouless crossover.

Secondly, the theory[8] predicts that the crossover occurs when the temperature-dependent phase-breaking length $L_\varphi(T)$ becomes of the order of the temperature-independent

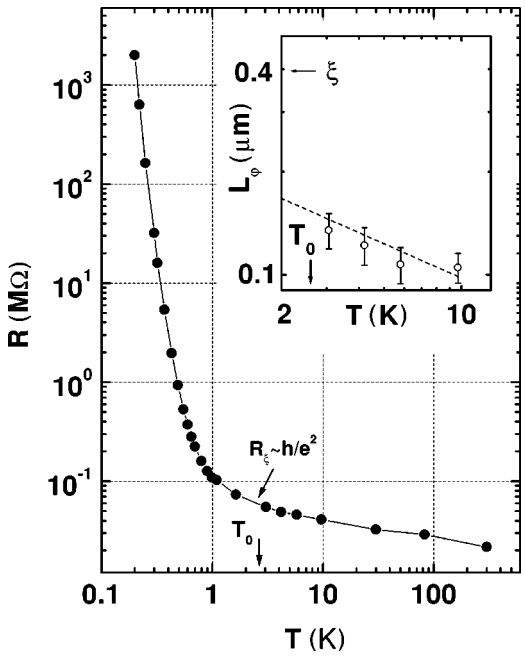

FIG. 1. The temperature dependence of the resistance of the 0.05-μm-wide wires (sample 1) in zero magnetic field without the gate, the solid curve is a guide to the eye. The arrow indicates the temperature T_0 that corresponds to the activation energy of hopping transport on the insulating side of the crossover. Inset: the temperature dependence of the phase-breaking length L_φ. The dashed line is the Nyquist phase-breaking length [Eq. (2)].

localization length. We estimated $L_\varphi(T)$ by fitting the high-temperature ($T>T_\xi$) magnetoresistance with the WL theory[24] (for a detailed procedure of fitting the experimental magnetoresistance of Q1D conductors with the theory,[21] see Refs. 20 and 24). It has been shown that the dominant phase-breaking mechanism in our samples on the metallic side of the crossover is the quasielastic electron-electron scattering;[21] both the temperature dependence of the phase-breaking length ($L_\varphi \sim T^{-1/3}$) and its magnitude are in a good agreement with the theoretical result (2).[24] For all the samples studied, L_φ at the crossover temperature is approximately 2–3 times smaller than ξ calculated from Eq. (1). However, it would be naive to expect the exact equality $L_\varphi(T_\xi)=\xi$ at $T=T_\xi$, since the prediction has an ''order-of-magnitude'' character.

The good agreement with Thouless' prediction indicates that in our samples the localization effects prevail in the WL-SL crossover. An additional evidence for that is provided by observation of the exponentially strong orbital magnetoresistance in the SL regime and the decrease of the crossover temperature in classically weak magnetic fields (see Sec. III C).

Thus, we observe the crossover from weak to strong localization in Q1D conductors as a function of temperature, when the electron states and disorder are *identical* on either side of the crossover. This important aspect of the experiment allows us to compare information on the electron states that can be obtained independently from the study of conductivity on *both sides* of the crossover.

III. THE STRONG LOCALIZATION REGIME

A. The temperature dependence of the resistance

On the insulating side of the crossover, an activated behavior of the resistance is observed (see Fig. 1): the experimental dependences $R(T)$ at $T \leqslant 0.3T_0$ can be fitted with the Arrhenius-type dependence

$$R(T)=R_0\exp\left(\frac{T_0}{T}\right). \tag{5}$$

Similar $R(T)$ dependences were reported earlier for the mesoscopic MOSFET-type structures in the SL regime.[1]

The experimental values of the activation energy k_BT_0 are very close to the spacing of the electron states on the scale of the localization domain Δ_ξ. We have verified this (a) by varying the width of samples, and (b) by varying the localization length with the gate voltage. In particular, Table I demonstrates that T_0 for the samples with the same diffusion constant varies proportional to W^{-2}, as one could expect from Eq. (3).

At the crossover temperature, *all relevant energy scales* become of the same order of magnitude:

$$\frac{\hbar}{\tau_\varphi(T_\xi)} \sim \Delta_\xi \sim \frac{\hbar D}{\xi^2} \sim k_BT_0 \sim k_BT_\xi. \tag{6}$$

Indeed, the scaling theory of localization[8,10] predicts that the crossover occurs when the smearing of the energy levels $\hbar/\tau_\varphi$ becomes comparable with the level spacing within the localization domain Δ_ξ. For a Q1D conductor, Δ_ξ is of the order of the Thouless energy, $\hbar D/\xi^2$ [Eq. (1)]. Our experimental data indicate that the activation energy k_BT_0 is also very close to the level spacing Δ_ξ (see below). Finally, if the Nyquist phase breaking is the dominant decoherence mechanism (which is always the case in low-dimensional conduc-

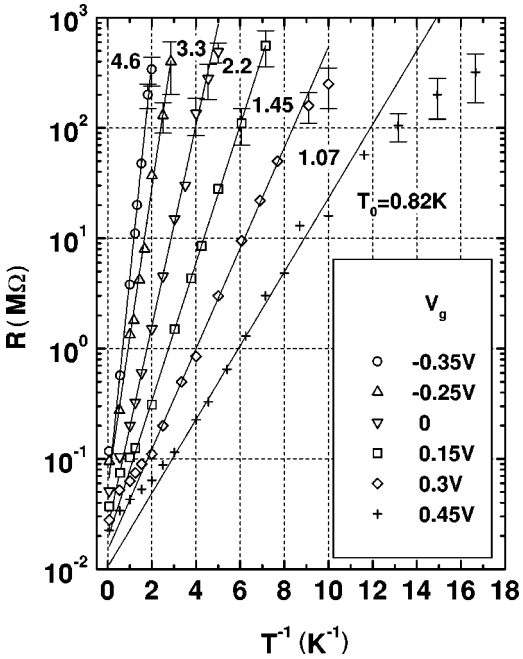

FIG. 2. The $R(T)$ dependences at different values of the gate voltage for sample 1. Straight lines are Arrhenius dependences (5) with the values of the activation energy T_0 shown next to the lines.

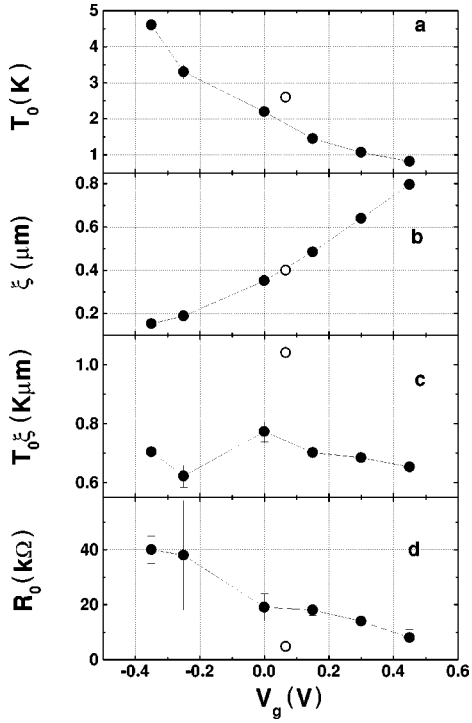

FIG. 3. The dependences of T_0, ξ, $T_0\xi$, and R_0 on the gate voltage for sample 1. Open dots are the corresponding values before the gate deposition. These values have been plotted at nonzero V_g to facilitate comparison of parameters for the samples with/without a gate with the *same* ξ. The values of ξ have been calculated from Eq. (1).

tors at sufficiently low temperatures), the phase-breaking rate $\hbar/\tau_\varphi$ becomes of the order of the temperature $T=T_\xi$ at the crossover [see Eqs. (1) and (2)]. In other words, the quasiparticle description holds over the *whole* temperature range that corresponds to the WL regime.[9]

Since the crossover temperature T_ξ and the temperature T_0 pertinent to the activation energy on the insulating side of the crossover are close to one another, we do not distinguish between them.[29] When discussing the crossover temperature in this paper, we refer to T_0, which can be accurately estimated on the insulating side of the crossover.

One can shift the crossover and vary the activation energy over a wide range by applying the gate voltage (the temperature dependences of the resistance for sample 1 at different V_g are shown in Fig. 2). With increasing the carrier concentration, the activation energy decreases [Fig. 3(a)] and the localization length increases [the values of ξ shown in Fig. 3(b) have been calculated from Eq. (1)]. However, the product $T_0\xi$ remains independent of the gate voltage [Fig. 3(c)]. Thus, the activation energy is inversely proportional to ξ. Numerically, the activation energy is very close to the mean energy spacing within the localization domain; we have also verified this by studying samples of different width (see Table I).

We observe correlation between the prefactor R_0 in the Arrhenius law (5) and the sheet resistance $R_\square$ on the metallic side of the crossover ($T\gg T_0$). For example, the magnitude of R_0 calculated for a segment of wire of the length ξ ($R_{0\xi}$) is 1.7 kΩ for sample 1 ($R_\square(20\ \mathrm{K})=1.6$ kΩ) and 12–14 kΩ for samples 3 and 5 [$R_\square(20\ \mathrm{K})=3.5$–$4.2$ kΩ]. The presence of the gate electrode affects $R_{0\xi}$: for sample 1, $R_{0\xi}$ has been increased up to 4 kΩ after the gate deposition. With increasing the gate voltage, R_0 decreases [Fig. 3(d)], however, $R_{0\xi}$ is almost V_g independent. This observation can be also presented as the V_g-independent ratio $R_0/R_\square(T\gg T_0)$ for a given sample. As will be shown below, the prefactor R_0 is not affected by the magnetic field.

The observed Arrhenius-type temperature dependence of the resistance with $k_BT_0\approx\Delta_\xi$ could be accounted for by different models of electron transport in the SL regime (see, e.g., Refs. 30–33). In particular, the theory of the variable range hopping (VRH) in one dimension[30,32,33] predicts the activation behavior of the resistance (in contrast to higher dimensions, where one can expect to observe either Mott's or Efros-Shklovskii law[34]). Similarity of the theoretical predictions stems from the fact that the resistance of a Q1D conductor is governed by the so-called *critical* hops, rare segments of a wire with no localized states in the vicinity of the Fermi level.[32,33] Indeed, any model of the SL transport that takes into account a realistic distribution of parameters of the hops, brings to the highly resistive hops separated by a distance L_c much larger than the hopping length. Thus, in order to test the relevance of different theoretical models to our experimental situation, we need to measure directly the two characteristic length scales: the hopping distance r_h for the critical hops, and the distance L_c between such hops. The experimental data on the hopping distance are still unavailable; without this information, it is difficult to distinguish between the alternatives: nearest-neighbor hopping versus variable-range hopping. We hope to address this problem in our future experiments with multiconnected samples fabricated from Q1D wires. However, the second important length scale, the distance between the critical hops, can be measured directly.

B. Nonlinearity of the *I*-*V* characteristics

The study of nonlinear effects in the SL regime allows one to measure L_C and its dependence on T and H, which is crucial for understanding of electron transport in the SL regime. For all the samples in Table I, we have measured the dependence of the resistance $R\equiv V/I$ on the voltage V across the sample at different temperatures; we have also repeated these measurements for sample 1 after the gate deposition for different V_g (all the data discussed in Sec. III A were obtained in the linear regime). The dependences $R(V)$ measured at different T and $H=0$ for sample 1 before the gate deposition are shown in Fig. 4.

Qualitatively, one can consider two different voltage regions for these dependences, separated by the characteristic voltage V^* ($\sim 5\times10^{-3}$ V for sample 1). At small $V<V^*$, the resistance is strongly temperature dependent; this voltage interval corresponds to the SL regime. For large $V>V^*$, all dependences $R(V,T)$ collapse onto a single curve regardless of the temperature; in the latter WL regime, the electron transport is nonactivated. Heating of sample 1 by measuring currents can be neglected at $V<1\times10^{-2}$ V: independent measurements show that the power 1 nW dissipated in the sample does not overheat electrons down to $T\sim0.1$ K.[35]

In the SL regime, the nonlinear resistance $R\equiv V/I$ for all samples can be fitted with the dependence:

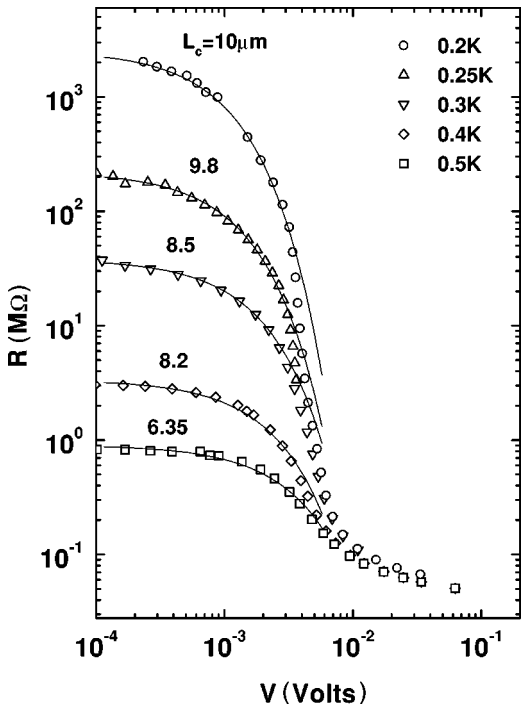

FIG. 4. The dependence of $R \equiv V/I$ on the voltage drop V across sample 1 at different temperatures (before the gate deposition). Solid curves are Eq. (7); the corresponding values of L_C in micrometers are shown next to each curve.

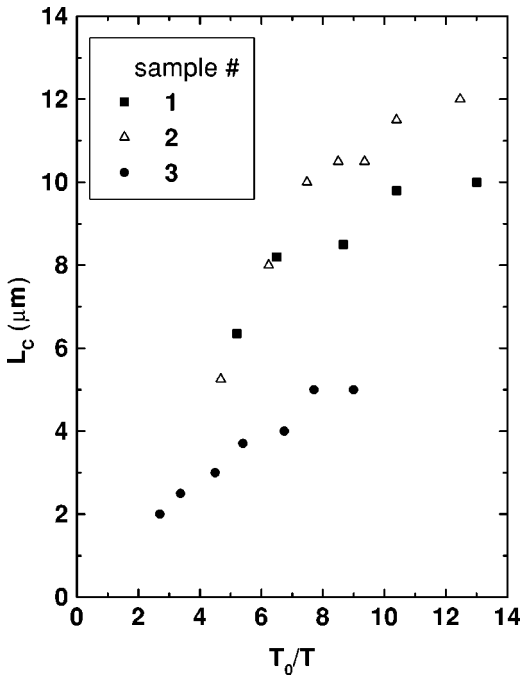

FIG. 5. The temperature dependence of L_C for different samples; the sample parameters are given in Table I.

$$R \sim \exp\left(\frac{T_0 - \alpha V}{T}\right), \tag{7}$$

where V is the total voltage across the sample. In order to clarify the physical meaning of α, we assume the following simplified model: the critical hops are identical, and they are separated by the average distance L_C, which is much greater than the hopping distance. In the electric field, the activation energy of each critical hop decreases proportionally to the voltage drop across the hop. In this model, α^{-1} is proportional to the average number of critical hops L/L_C in a wire of the length L.

Obviously, this model is very naive. However, a more realistic model based on the normal distribution of the activation energies and self-consistent calculation of the voltage drop across each hop fits the experimental dependences $R(V)$ less accurately than Eq. (7).

On the basis of this model, one can estimate the distance between the critical hops $L_C = \alpha L k_B/e$. This distance increases with decreasing the temperature (Fig. 5) and at $T_0/T \gg 1$ it exceeds ξ by more than an order of magnitude. However, even at the lowest temperatures, this distance is still a factor of ~ 50 smaller than the total length of the wire.

The theory[33] predicts that the wire-to-wire fluctuations can be neglected if $\eta \equiv \ln(L/\xi)/\ln(L_C/\xi) > 1$; for our experimental values of L_C, $\eta = 2-3$ for all T and V_g for all samples. Since the width of the distribution function for the wire's resistance depends exponentially on η, the wire-to-wire fluctuations are averaged out in our ''long'' samples. Thus, the wire resistance is a *self-averaged* quantity in the studied temperature range (the resistance fluctuations decrease with increasing the wire length). The opposite case of large fluctuations in mesoscopic samples ($L \leqslant L_C$) has been studied by Hughes *et al.*[36]

Another experimental evidence for the self-averaged behavior of the wire resistance stems from comparison of the samples comprising 5 wires with $L = 40$ μm and 470 wires with $L = 500$ μm. For 40 μm-long wires we observed resistance fluctuations in strong magnetic fields (Fig. 9; see also Ref. 22); these fluctuations are completely washed out for longer wires (Fig. 8). Relatively small values of L_C are also consistent with the fact that we have not observed any rectifying effects even for the 40-μm-long wires; the rectifying effects are typical for mesoscopic samples.[1]

The study of L_C for the same sample at different V_g shows that L_C is *proportional* to ξ for a fixed T_0/T. For sample 1 both L_C and ξ increase with increasing V_g by a factor of ~ 6, however, the ratio L_C/ξ remains the same for all V_g (Fig. 6).

The temperature dependences of L_C shown in Fig. 5 contradict the VRH theory in one dimension, which predicts the exponential temperature dependence of L_C,[32,33]

$$L_C = \xi \sqrt{\frac{T_0}{T}} \exp\left(\frac{T_0}{2T}\right). \tag{8}$$

Instead, L_C grows approximately as T_0/T at high temperatures and saturates at lower T (Fig. 5). This discrepancy remains the challenge for the theory.

C. The magnetoresistance

An important advantage of our experiment is that we can measure directly the localization length by studying the magnetoresistance in the SL regime. The magnetoresistance for sample 1 below the crossover temperature is shown in Fig. 7. The magnetoresistance in the WL and SL regimes shares

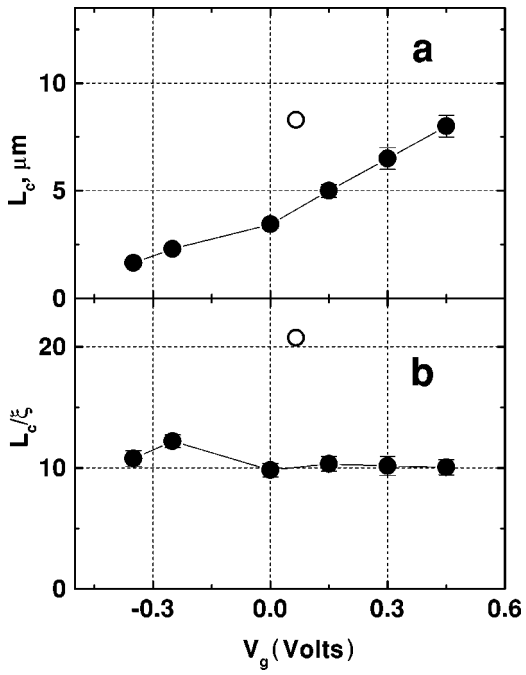

FIG. 6. (a) The dependence of L_C on V_g at a fixed $T_0/T \simeq 8.25$. (b) The ratio L_C/ξ vs V_g. The open circles correspond to the measurements before the gate deposition.

several common features: it is negative and strongly anisotropic (this pure orbital magnetoresistance vanishes for the parallel orientation of the field with respect to the plane of the δ layer). However, the magnitude of the magnetoresistance increases dramatically on the insulating side of the crossover. The inset in Fig. 7 demonstrates that the crossover

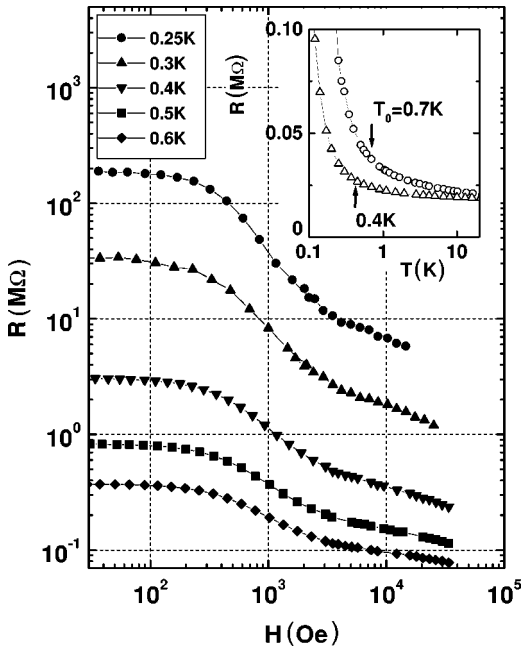

FIG. 7. The magnetoresistance of sample 1 without the gate electrode at different temperatures ($T \ll T_0 = 2.6$ K). The solid lines are guides to the eye. The inset: the shift of the crossover in the magnetic field for the same sample with the gate electrode at $V_g = +0.7$ V (○: $H=0$; △: $H=17$ kOe).

shifts down to lower temperatures, and the magnetoresistance becomes exponentially strong in classically weak magnetic fields.

For different fixed values of the magnetic field, we observe the exponential temperature dependence of the resistance with the same prefactor R_0. The *only* parameter that varies with the magnetic field is the activation energy:

$$R(T,H) = R_0 \exp[T_0(H)/T]. \tag{9}$$

Thus, the magnetoresistance is due to the magnetic field dependence of the activation energy.[22,23] Taking this into account, it is convenient to convert the magnetoresistance into the H dependence of the activation energy:

$$\frac{T_0(H)}{T_0(H=0)} = \frac{T}{T_0(H=0)} \ln \frac{R(H)}{R_0}. \tag{10}$$

The dependences (10) measured for samples 1 and 5 at different temperatures $T \ll T_0$ are shown in Figs. 8 and 9. For all the samples, these dependences collapse onto the *same universal* curve, which reflects the transition from weak to strong fields; the normalized activation energy varies between 1 ($H=0$) and ~ 0.5 (strong fields). (For samples with $L = 40$ μm, the deviations from this universal curve due to insufficient averaging of mesoscopic fluctuations have been observed in strong fields,[22] see Fig. 9.)

It was shown in Sec. III A that the activation energy in our samples practically coincides with the mean energy spacing within the localization domain and is inversely proportional to the localization length. Thus, the observed magnetoresistance reflects the universal magnetic-field dependence of the localization length.

This observation is in agreement with the theoretical prediction that the localization length in a 1D conductor with a large number of channels N_{1D} should be a universal function of the symmetry class:[11,37–39]

$$\xi = \gamma N_{1D} l, \tag{11}$$

where $\gamma = 2\beta/s$, β is the Dyson parameter, which characterizes the symmetry properties of the system, and s is the Kramers degeneracy of the channels. The coefficient γ equals 1(2,4,4), respectively, for potential scattering ($\beta=1$, $s=2$), potential scattering in strong magnetic field ($\beta=2$, $s=2$), spin-flip scattering by magnetic impurities *or* the strong spin-orbit scattering in strong magnetic field ($\beta=2$, $s=1$, note broken Kramers degeneracy), and the strong SO scattering at $H=0$ ($\beta=4$, $s=2$). In our case, the magnetic field induces a transition from the orthogonal to unitary case without breaking the spin degeneracy of the scattering channels ($\beta=1$, $s=2 \rightarrow \beta=2$, $s=2$) and, hence, *doubling* of ξ. The theory is well adapted to the conductors with a large localization length, where electrons move diffusively within the localization domain. Since for our samples $T_0 \simeq \Delta_\xi \sim 1/\xi$, *doubling* of the localization length should result in *halving* the activation energy in agreement with our experimental data.

Figure 8 shows that the activation energy for sample 1 diminishes in strong magnetic fields less than by a factor of 2. We believe that two reasons preclude observation of the *exact* halving of T_0 in this sample. First, the number of chan-

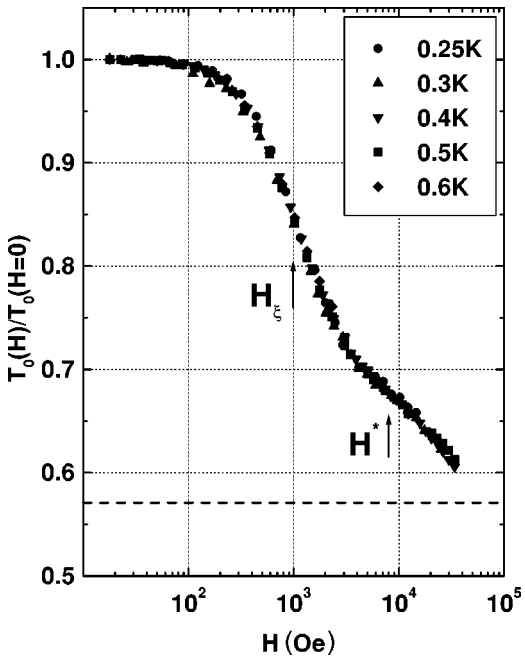

FIG. 8. The normalized magnetic field dependences of the activation energy for sample 1. Characteristic fields H_ξ and H^* are shown with arrows. The dashed line is the theoretical strong-field limit for $N_{1D}=7$ (see the text).

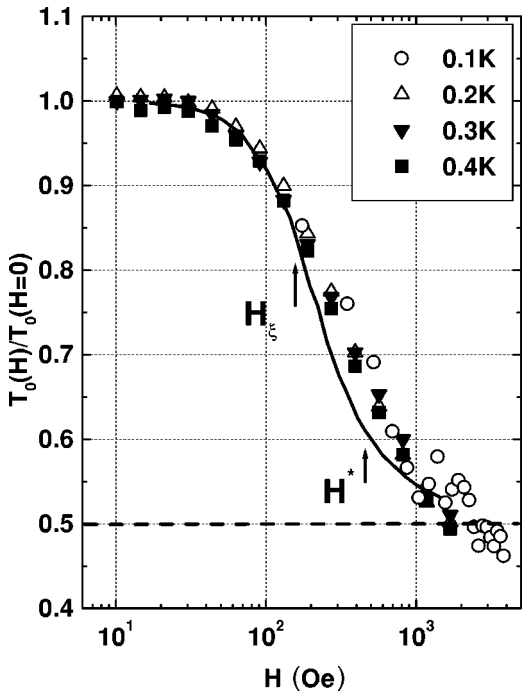

FIG. 9. The normalized magnetic field dependences of the activation energy for sample 5. The solid line is the theoretical dependence $\xi(0)/\xi(H)$ $[=T_0(H)/T_0(0)]$ for $N_{1D}\gg 1$ (see the text). The dashed line is the theoretical strong-field limit. The amplitude of reproducible fluctuations of magnetoresistance, observed at $H \geqslant 1$ kOe, increases with the decrease of temperature; the fluctuations clearly manifest themself at $T=0.1$ K.

nels is not very large for sample 1 ($N_{1D}\simeq 7$); in this case, the exact expression for ξ should be used ($s=2$):[39]

$$\xi=(\beta N_{1D}+2-\beta)l. \tag{12}$$

According to Eq. (12), for a conductor with $N_{1D}=7$, T_0 in strong fields should be smaller than $T_0(H=0)$ by a factor of 1.75. The corresponding high-field limit of T_0 is shown as the dashed line in Fig. 8. Note that for sample 5 with a large number of transverse channels ($N_{1D}\simeq 30$), the normalized T_0 approaches the level 0.5 in strong fields (Fig. 9). Secondly, in stronger fields $H>H^*=\Phi_0/W^2$ (Φ_0 is the magnetic flux quantum), two essential requirements of the theory applicability are violated: sample 1 becomes two dimensional with respect to the localization effects, and, at the same time, transport is already affected by the magnetic field at scales smaller than the mean free path (since l is close to W for this sample). In this case, the dependence $\xi(\beta)$ is more complicated and not universal.[40,41]

Not only the limits of variation of $\xi(H)$ are in agreement with the theory, but also the shape of the transition curve in the field range $H<H^*$ is consistent with the analytical expression for $\xi(H)$ obtained for all magnetic fields by Bouchaud.[40] The dependence $\xi(H)$ calculated for $N_{1D}\gg 1$ is shown in Fig. 9 by the solid curve. In particular, our data are consistent with the prediction that the limit $\xi(H)/\xi(0)$ is reached slowly with increasing H.[40]

Our experiments[22–24] provide evidence of the doubling of ξ due to breaking of the time-reversal symmetry. Previously, the idea of the universal change of ξ in magnetic fields has been used for interpretation of the magnetoresistance of several 2D and 3D systems with variable-range hopping.[37,42,43] Although the effects in higher dimensions could be qualitatively similar, the doubling of ξ is expected only in the Q1D geometry.[40,41] It is unclear at present how to reconcile the observed positive magnetoresistance in insulating 1D samples with strong SO scattering,[42] with the theory that properly accounts for Kramers degeneracy.[44,45] In this case, the magnetic field should not affect the localization length, since the time-reversal symmetry and Kramers degeneracy are broken simultaneously.[11,44,45]

Observation of the magnetic-field-induced doubling of ξ provides us with a *direct* method of measurement of ξ in Q1D conductors. Indeed, the localization length is the only unknown parameter in fitting the experimental dependences $T_0(H)/T_0$ with the theory.[40] According to the theory,[40] $T_0(H)/T_0(H=0)\approx 0.83$ in the characteristic field

$$H_\xi=\frac{\Phi_0}{\xi W}, \tag{13}$$

which corresponds to breaking of the time-reversal symmetry within the localization domain.[46] The value of H_ξ for samples 1 and 5 are shown by arrows in Figs. 8 and 9. For all the samples studied, the experimental values of ξ are in an excellent agreement with the estimate of the localization length from the resistance in the ''metallic'' regime (1) (see Table I).

The evolution of the $R(V)$ dependences with magnetic field for sample 1 is shown in Fig. 10. In the SL regime ($V \ll V^*$), these normalized dependences are not affected by the magnetic field in accord with our experimental observation that $L_C\sim\xi(T_0/T)=1/\nu_{1D}T$. However, the values of V, where deviation from the fitting curve (7) is observed, are

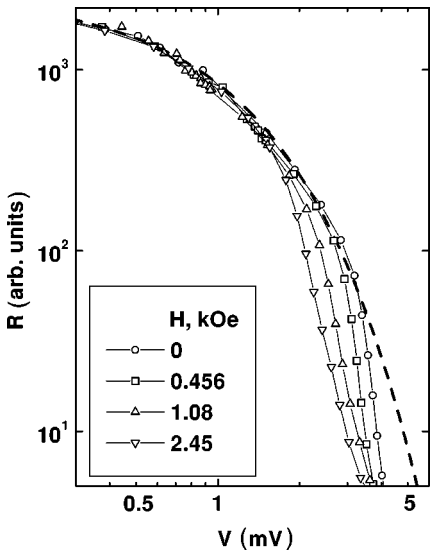

FIG. 10. The normalized $R(V)$ dependences at different H, $T=0.2$ K. Solid lines are guides to the eye; the dashed line denotes Eq. (7).

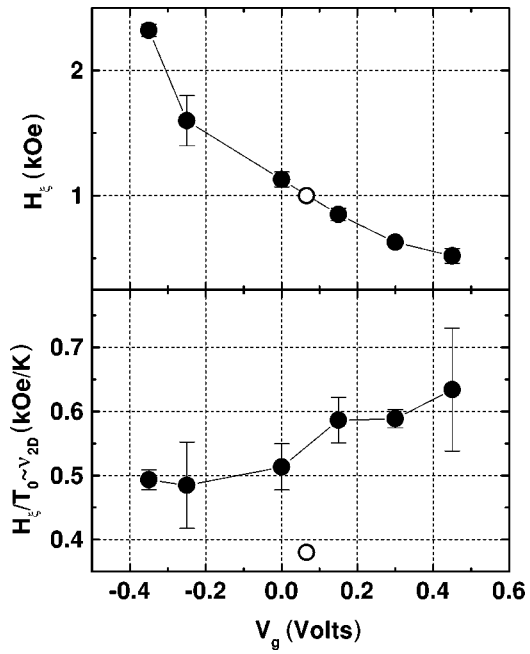

FIG. 11. The dependence of H_ξ and ν_{2D} on V_g. Solid lines are guides to the eye. Open circles correspond to the values before the gate deposition.

diminishing with the increase of magnetic field. We cannot suggest a plausible explanation of this experimental fact.

D. The density of states

Comparison of expressions for the activation energy $k_B T_0 \approx \Delta_\xi$ and the characteristic field H_ξ shows that the ratio of these quantities depends only on the single-particle density of states:

$$\frac{H_\xi}{\Delta_\xi} = \frac{\Phi_0 \nu_{1D}}{W} = \Phi_0 \nu_{2D}. \tag{14}$$

Thus, by measuring the experimental counterpart of this ratio, H_ξ^{expt}/T_0, one can probe the DOS at the energy scale $\sim k_B T_0$ near the Fermi level. The values of H_ξ^{expt}/T_0 for samples without a gate are listed in Table I. Despite of an order-of-magnitude variation of H_ξ and T_0 for different samples, their ratio remains close to the estimate 0.5 kOe/K, obtained for the noninteracting electrons in the parabolic conduction band ($\nu_{2D} = m^*/\pi\hbar^2$, $m^* = 0.067_e$).

Interestingly, however, we observe $\sim 40\%$ increase of ν_{2D} after *deposition* of the gate electrode (Fig. 11). The increase of ν_{2D} also manifests itself in the decrease of T_0 (Fig. 3) and increase of L_C (Fig. 6) if one compares the samples with the same localization length. This behavior of ν_{2D} is difficult to explain in the model of noninteracting electrons. We believe that this is a manifestation of the effect of the *long-range* Coulomb interaction on the DOS in the SL regime. Indeed, the Coulomb interaction, being poorly screened in Q1D conductors, can affect both thermodynamic and transport properties. In particular, Raikh and Efros predicted a logarithmic singularity of the single-particle DOS at the Fermi energy in Q1D conductors in the SL regime:[47]

$$\nu_{1D}(\varepsilon) = \frac{\nu_{1D}^0}{1 + (e^2 \nu_{1D}^0/K) \ln(\varepsilon_\xi/\varepsilon)}, \tag{15}$$

where ν_{1D}^0 is the ''nucleating'' DOS, K is the relative permittivity of the medium around the conductor, and ϵ_ξ gives a measure of the strength of nearest-neighbor interaction. Suppression of the long-range Coulomb interaction can result in the measurable increase of ν_{2D}. Indeed, deposition of the gate electrode ''screens'' the long-range part of the Coulomb interaction: it becomes of a dipole-dipole type at distances greater than the distance t between the electron gas and the metallic gate electrode (for our samples, $t = 0.1$ μm is much smaller than ξ and the hopping length). To the best of our knowledge, this is the first experimental evidence of the minimum of the DOS at the Fermi level in Q1D conductors. This could also be an indirect evidence that the hopping distance at $T \ll T_0$ exceeds ξ: only in this case one can expect to observe the effect of the Coulomb interaction on the DOS.

IV. CONCLUSION

In conclusion, we have studied the resistance of quasi-one-dimensional wires fabricated from Si δ-doped GaAs as a function of temperature, magnetic field, and applied voltage. The crossover from weak to strong localization has been observed in these conductors with decreasing temperature. The main features of the observed crossover, driven by both localization and interaction effects, are in agreement with the Thouless scenario: the crossover occurs when the phase-breaking length becomes comparable with the localization length, and the resistance of the segment of wire of the length ξ is $\sim h/e^2$.

On the insulating side of the crossover, we observe the activation temperature dependence of the resistance with the activation energy very close to the mean energy spacing within the localization domain. Both the crossover temperature and the activation energy can be varied over a wide range by the gate voltage.

The study of nonlinearity of the current-voltage characteristics in the SL regime provides the direct measurement of the distance between the critical electron hops, which govern the resistance of a Q1D conductor. This distance L_c is proportional to the localization length; it increases with decreasing temperature, and at low temperatures ($T/T_0=0.1$) exceeds ξ by a factor of ~ 30. However, L_c is insufficiently large to be consistent with prediction of the theory of variable range hopping in Q1D conductors.[32,33] Since L_c is much smaller than the length of wires, there is no rectifying effects in the resistance of our samples, and the wire-to-wire fluctuations of the resistance are negligible.

The exponentially strong magnetoresistance in the SL regime is due to the magnetic field dependence of the localization length. Observation of the universal magnetic-field dependence of the activation energy, which is caused by breaking of time-reversal symmetry in strong fields, has been used for the direct measurement of ξ in Q1D conductors. There is good agreement between the values of ξ estimated from the SL magnetoresistance and calculated from the resistance in the WL regime.

Simultaneous measurement of the activation energy and the characteristic field of doubling of the localization length allows one to probe the single-particle density of states at the Fermi level in Q1D conductors. Our data indicate that deposition of the gate electrode decreases the amplitude of the minimum. We believe that this is due to screening of the long-range interaction by the metal film separated from the Q1D conductor by a distance much smaller than the hopping length.

In the situation when direct measurement of the hopping distance is still unavailable, it is difficult to give preference to one of the models of electron transport in the insulating regime (nearest-neighbor hopping versus variable-range hopping). However, observation of the minimum of the density of states at the Fermi level can serve as an indirect evidence that the hopping distance exceeds the localization length. More theoretical efforts are needed to take into account such essential features of quasi-one-dimensional conductors as strong overlapping between the localized electron states and long-range Coulomb interaction.

ACKNOWLEDGMENTS

We are grateful to our collaborators, A. G. Mikhalchuk and H. M. Bozler; their help was essential at the initial stage of this work. It is our pleasure to thank I. L. Aleiner, B. L. Altshuler, A. I. Larkin, A. D. Mirlin, M. E. Raikh, and B. I. Shklovskii for helpful discussions. We are grateful to B. K. Medvedev for fabrication of the δ-doped GaAs layers.

[1] A. B. Fowler, J. J. Wainer, and R. A. Webb, in *Hopping Transport in Solids*, edited by M. Pollak and B. Shklovskii (North-Holland, Amsterdam, 1991) p. 233; A. Kastner, R. F. Kwasnick, J. C. Licini, and D. J. Bishop, Phys. Rev. B **36**, 8015 (1987).

[2] For recent references, see V. N. Prigodin and K. B. Efetov, Phys. Rev. Lett. **70**, 2932 (1993); R. S. Kohlman *et al.*, *ibid.* **78**, 3915 (1997); J. Joo *et al.*, Phys. Rev. B **57**, 9567 (1998); M. Ahlskog *et al.*, *ibid.* **55**, 6777 (1997); A. Aleshin *et al.*, *ibid.* **56**, 3659 (1997).

[3] T. W. Ebbesen *et al.*, Nature (London) **382**, 54 (1996); S. J. Tans *et al.*, *ibid.* **386**, 474 (1997); A. Bezryadin *et al.*, Phys. Rev. Lett. **80**, 4036 (1998).

[4] J. Voit, Rep. Prog. Phys. **57**, 977 (1995).

[5] H. Maurey and T. Giamarchi, Phys. Rev. B **51**, 10 833 (1995).

[6] H. L. Schulz, in *Mesoscopic Quantum Physics*, edited by E. Akkermans *et al.* (Elsevier, Amsterdam, 1994).

[7] A. O. Gogolin, Ann. Phys. (Paris) **19**, 977 (1994).

[8] D. J. Thouless, Phys. Rev. Lett. **39**, 1167 (1977); Solid State Commun. **34**, 683 (1980).

[9] B. L. Altshuler and A. G. Aronov, in *Electron-Electron Interactions in Disordered Systems*, edited by M. Pollak and A. L. Efros (North-Holland, Amsterdam, 1985) p. 1.

[10] E. Abrahams, P. W. Anderson, D. C. Licciardello, and T. V. Ramakrishnan, Phys. Rev. Lett. **42**, 673 (1979).

[11] K. B. Efetov and A. I. Larkin, Zh. Eksp. Teor. Fiz. **85**, 764 (1983) [Sov. Phys. JETP **58**, 444 (1983)]; O. N. Dorokhov, *ibid.* **85**, 1040 (1983) [*ibid.* **58**, 606 (1983)].

[12] Y. Imry, *Introduction to Mesoscopic Physics* (Oxford University Press, New York, Oxford, 1997).

[13] Y. Imry and Z. Ovadyahu, J. Phys. C **15**, L327 (1982); Z. Ovadyahu and Y. Imry, *ibid.* **16**, L471 (1983).

[14] H. White and G. Bergmann, Phys. Rev. B **40**, 11 594 (1989).

[15] F. W. Van Keuls, H. Mathur, H. W. Jiang, and A. J. Dahm, Phys. Rev. B **56**, 13 263 (1997).

[16] S.-Y. Hsu and J. M. Valles Jr., Phys. Rev. Lett. **74**, 2331 (1995).

[17] T. J. Thornton, M. Pepper, H. Ahmed, D. Andrews, and G. J. Davies, Phys. Rev. Lett. **56**, 1198 (1986).

[18] R. G. Mani, K. von Klitzing, and K. Ploog, Phys. Rev. B **48**, 4571 (1993).

[19] S. Wind, M. J. Rooks, V. Chandrasekhar, and D. E. Prober, Phys. Rev. Lett. **57**, 633 (1986).

[20] P. M. Echternach, M. E. Gershenson, H. M. Bozler, A. L. Bogdanov, and B. Nilsson, Phys. Rev. B **48**, 11 516 (1993).

[21] B. L. Altshuler, A. G. Aronov, and D. E. Khmelnitskii, J. Phys. C **15**, 7357 (1982).

[22] M. E. Gershenson, Yu. B. Khavin, A. G. Mikhalchuk, H. M. Bozler, and A. L. Bogdanov, Phys. Rev. Lett. **79**, 725 (1997).

[23] Yu. B. Khavin, M. E. Gershenson, and A. L. Bogdanov, Usp. Fiz. Nauk. **168**, 200 (1998) [Phys. Usp. **41**, 186 (1998)].

[24] Yu. B. Khavin, M. E. Gershenson, and A. L. Bogdanov, Phys. Rev. Lett. **81**, 1066 (1998).

[25] K.-F. Berggren, G. Roos, and H. van Houten, Phys. Rev. B **37**, 10 118 (1988).

[26] G.-Q. Hai, N. Studart, and F. M. Peeters, Phys. Rev. B **52**, 8363 (1995).

[27] S. Schuppler *et al.*, Phys. Rev. B **51**, 10 527 (1995).

[28] T. Schmidt *et al.*, Phys. Rev. B **54**, 13 980 (1996).

[29] Because all the relevant energies are of the same magnitude at the crossover, the *power-law* temperature dependence of the conductivity, $\sigma \sim \tau_\varphi^{-1} \sim T^p$, that has been suggested for the temperature range $T_0 < T < T_\xi$ (Refs. 12 and 17) cannot be observed in 1D conductors with the dominant Nyquist phase breaking.

[30] J. Kurkijarvi, Phys. Rev. B **8**, 922 (1973).

[31] A. I. Larkin and D. E. Khmelnitskii, Zh. Eksp. Teor. Fiz. **83**, 140

(1982) Sov. Phys. JETP **56**, 647 (1982).

[32] P. A. Lee, Phys. Rev. Lett. **53**, 2042 (1984); R. A. Serota, R. K. Kalia, and P. A. Lee, Phys. Rev. B **33**, 8441 (1986).

[33] M. E. Raikh and I. M. Ruzin, Zh. Eksp. Teor. Fiz. **95**, 1113 (1989) [Sov. Phys. JETP **68**, 642 (1989)].

[34] B. I. Shklovskii and A. L. Efros, *Electronic Properties of Doped Semiconductors* (Springer-Verlag, Berlin, 1984).

[35] The resistance of the GaAs layer between the gate electrode and the electron gas in our samples is strongly nonlinear: for sample 1, this resistance R_g is very large at $V_g < 0.5$ V, however, starting with $V_g \sim 0.5$ V, it decreases with increasing V_g down to 0.5 GΩ at $V_g = 2$ V. For this reason, all the measurements have been performed at $V_g < 0.5$ V. The power $P = V_g^2/R_g$, which is dissipated in the sample, is 1 nW at $V_g = 1$ V; this power does not affect the electron temperature down to 0.1 K.

[36] R. J. F. Hughes *et al.*, Phys. Rev. B **54**, 2091 (1996).

[37] J.-L. Pichard, M. Sanquer, K. Slevin, and P. Debray, Phys. Rev. Lett. **65**, 1812 (1990).

[38] Y. V. Fyodorov and A. D. Mirlin, Phys. Rev. Lett. **67**, 2405 (1991).

[39] C. W. J. Beenakker, Rev. Mod. Phys. **69**, 731 (1997).

[40] J. P. Bouchaud, J. Phys. I **1**, 985 (1991); J. P. Bouchaud and D. Sornette, Europhys. Lett. **17**, 721 (1992).

[41] I. V. Lerner and Y. Imry, Europhys. Lett. **29**, 49 (1995).

[42] P. Hernandez and M. Sanquer, Phys. Rev. Lett. **68**, 1402 (1992).

[43] F. Ladieu *et al.*, J. Phys. I **3**, 2321 (1993).

[44] Y. Meir, N. S. Wingreen, O. Entin-Wohlman, and B. L. Altshuler, Phys. Rev. Lett. **66**, 1517 (1991).

[45] A. D. Mirlin, Phys. Rev. Lett. **72**, 3437 (1994).

[46] In our previous papers,[23,24] we extracted the values of H_ξ by fixing the level $T_0(H_\xi) = 0.85T_0(0)$ [at that time we were unaware of the calculations (Ref. 40)]. This choice was based on comparison of the experimental data for many samples with the theoretical estimate for H_ξ. The calculated values of H_ξ were in an excellent agreement with the experimental ones; this indicates that the shape of the transition curve is the same for all the samples.

[47] M. E. Raikh and A. L. Efros, Pis'ma Zh. Eksp. Teor. Fiz. **45**, 225 (1987) [JETP Lett. **45**, 280 (1987)].